Article title: Feedbacks between plant N demand and rhizosphere priming depend on type of mycorrhizal association

Running title: Modeling plant-soil mycorrhizal feedbacks

Keywords: mycorrhizae, carbon cycling, plant-soil interactions, soil carbon, N-cycle feedbacks, forest productivity, biogeochemical model, biogeochemistry

Authors:
Benjamin N. Sulman: Program in Atmospheric and Oceanic Sciences, Department of Geosciences, Princeton University, Princeton, New Jersey, USA, bsulman@princeton.edu
Edward R. Brzostek: Department of Biology, West Virginia University, Morgantown, West Virginia, USA, erbrzostek@mail.wvu.edu
Chiara Medici: Princeton Environmental Institute, Princeton University, Princeton, New Jersey, USA, chiaramed2@gmail.com
Elena Shevliakova: NOAA Geophysical Fluid Dynamics Laboratory, Princeton, New Jersey, USA, elena.shevliakova@noaa.gov
Duncan N. L. Menge: Department of Ecology, Evolution, and Environmental Biology, Columbia University, New York, New York, USA, dm2972@columbia.edu
Richard P. Phillips: Department of Biology, Indiana University, Bloomington, Indiana, USA, rpp6@indiana.edu

Corresponding author: Benjamin Sulman: bsulman@princeton.edu. Phone: (608) 332-0047. Fax: (609) 987-5063. Mail: 201 Forrestal Road, Princeton, NJ 08540, USA.

Statement of Authorship: BNS conducted model simulations. BNS, RPP, and ERB analyzed model results. ERB collected and analyzed field measurements, and RPP contributed to conceptualization and design of observations. BNS, ERB, and CM wrote model code, and ES and DM contributed to model design. BNS and ERB wrote the initial manuscript text, and all coauthors contributed to revisions.

Data accessibility: Field measurements used for model simulations are included as supplementary material. Model code is archived on GitHub (https://github.com/bsulman/FUN-CORPSE) and model output is archived on Figshare (doi 10.6084/m9.figshare.5016383 and 10.6084/m9.figshare.5016377).

Type of article: Letters

Number of words:
Abstract: 150
Main text: 5018
Number of references: 45
Number of figures: 6
Number of tables: 0
Number of text boxes: 0

Abstract:

Ecosystem carbon (C) balance is hypothesized to be sensitive to the mycorrhizal strategies that plants use to acquire nutrients. To test this idea, we coupled an optimality-based plant nitrogen (N) acquisition model with a microbe-focused soil organic matter (SOM) model. The model accurately predicted rhizosphere processes and C-N dynamics across a gradient of stands varying in their relative abundance of arbuscular mycorrhizal (AM) and ectomycorrhizal (ECM) trees. When mycorrhizal dominance was switched – ECM trees dominating plots previously occupied by AM trees, and vice versa – legacy effects were apparent, with consequences for both C and N stocks in soil. Under elevated productivity, ECM trees enhanced decomposition more than AM trees via microbial priming of unprotected SOM. Collectively, our results show that ecosystem responses to global change may hinge on the balance between rhizosphere priming and SOM protection, and highlight the importance of dynamically linking plants and microbes in terrestrial biosphere models.

1. Introduction

Nutrient availability plays a central role in the degree to which ecosystems store carbon (C), but there is substantial uncertainty about the importance of this effect under changing climate and rising atmospheric CO_2 levels (Friedlingstein *et al.* 2006; Heimann & Reichstein 2008). In terrestrial biosphere models (TBMs), land C sinks can exceed independently-derived estimates of nitrogen (N) availability (Hungate *et al.* 2003; Wieder *et al.* 2015), casting doubt on the ability of "C only" TBMs to project C cycle-climate feedbacks. While more TBMs have begun to include N dynamics, most of these models represent soil N availability independently from plant N acquisition strategies, and do not consider the ability of plants to actively influence microbial communities and biogeochemical cycles to meet their N demand (Finzi *et al.* 2015; Thomas *et al.* 2015). Observations suggest that roots stimulate soil N cycling by releasing C into the rhizosphere either as root exudates or as direct transfers to mycorrhizal fungi. This accelerates soil organic matter (SOM) turnover by enhancing microbial growth and extracellular enzyme production (Kuzyakov 2010; Phillips *et al.* 2011; Phillips *et al.* 2012). However, this ability of plants to accelerate SOM turnover remains largely absent from TBMs, representing an important gap between our mechanistic and predictive understanding of the terrestrial C sink.

There is emerging evidence that the mycorrhizal associations of plants in a given community both determine and reflect ecosystem N cycling and related feedbacks to global changes (Phillips *et al.* 2013; Lin *et al.* 2016; Terrer *et al.* 2016). Trees associating with ECM fungi typically have leaf litter that decomposes slower than that of AM-

86 associated trees (Cornelissen *et al.* 2001; Midgley *et al.* 2015). Consequently, N cycling
87 rates, on average, are slower in ECM stands than AM stands (Lin *et al.* 2016). However,
88 these low rates of N cycling do not appear to limit ECM plants' ability to enhance their
89 growth in response to elevated CO_2. Across a global synthesis of over 80 elevated CO_2
90 experiments, Terrer *et al.* (2016) found that when N was limiting, ECM plants were able
91 to achieve biomass gains under elevated CO_2 that were not realized by AM plants.
92 Moreover, in forests, these biomass gains were facilitated not by increased N use
93 efficiency but by enhanced N uptake (e.g. Finzi *et al.* 2007; Drake *et al.* 2011; Zaehle *et*
94 *al.* 2014). These findings raise a critical question: If N cycling is slower in ECM soils,
95 how do ECM (but not AM) plants accelerate N uptake under elevated CO_2?
96
97 One plausible explanation concerns interactions between priming effects on SOM cycling
98 and the dominant modes of SOM stabilization, both of which differ between ECM- and
99 AM-dominated forests. ECM fungi are thought to produce extracellular enzymes that
100 promote decomposition of N-bearing organic compounds, while AM fungi generally rely
101 on uptake of inorganic N (Read & Perez Moreno 2003, but see Pelletier and Zak, 2017).
102 Further, rapidly decomposing AM leaf and root litter may promote more physically
103 protected N accumulation given that rapid litter decay enhances the production of N-rich
104 microbial necromass that becomes stabilized on soil mineral surfaces (Cotrufo *et al.*
105 2013). By contrast, ECM litter decays more slowly, producing larger stocks of organic N
106 in forms that are energetically demanding to decompose but not physically protected, and
107 therefore more vulnerable to priming effects (Kuzyakov 2010). While both theory and
108 observations support the above framework (e.g. Phillips *et al.* 2013; Averill *et al.* 2014),

109 the relative roles of priming effects and physical protection in ecosystem responses to
110 global change remain unclear. Due to the complexity of these interactions, ecosystem
111 modeling is a key tool for examining these processes.
112
113 Here, we present a novel modeling framework that couples mycorrhizal-specific patterns
114 of C allocation and N demand with soil microbial decomposition and physico-chemical
115 stabilization of SOM. We coupled two state-of-the-art models that are currently
116 implemented in global scale TBMs: (1) the Fixation and Uptake of Nitrogen (FUN)
117 Model (Fisher *et al.* 2010; Brzostek *et al.* 2014b; Shi *et al.* 2016) and (2) the Carbon,
118 Organisms, Rhizosphere, and Protection in the Soil Environment (CORPSE) model
119 (Sulman *et al.* 2014). FUN predicts vegetation N demand and the resulting allocation of
120 C to N acquisition via mycorrhizae and root exudation. CORPSE predicts the formation
121 and decomposition of SOM, explicitly including microbial activity and physical
122 protection. We validated the coupled model, FUN-CORPSE, against measurements
123 across a gradient from AM-dominant to ECM-dominant forest stands in southern Indiana,
124 USA. We then used the model to address three major questions: (1) To what degree do
125 plant traits connected with different mycorrhizal associations interact with physical
126 protection and priming effects to determine patterns of SOM storage? (2) To what degree
127 do shifts in the dominant mycorrhizal association affect soil C and N dynamics? (3) To
128 what degree do differences in plant traits and soil properties between mycorrhizal types
129 affect ecosystem responses to increases in net primary productivity, such as those driven
130 by elevated CO_2?
131

We show that FUN-CORPSE accurately captures observed patterns of biogeochemical cycling across the mycorrhizal gradient. Model simulations suggest that (1) ECM-associated stands store more SOM in chemically resistant pools while AM-dominated stands store more SOM in physically protected pools; (2) physical protection of SOM drives legacy effects of mycorrhizal dominance that can influence soil N availability and C storage for decades; and (3) under increasing productivity (as expected from elevated CO_2), ECM stands accelerate the mobilization of N from SOM to a greater extent than AM stands. Collectively, these results highlight the tight couplings between plant traits, modes of SOM stabilization, and the capacity of vegetation to accelerate SOM turnover.

2. Methods

2.1. Nitrogen acquisition model

We estimated plant N demand and rhizosphere C allocation using the Fixation and Uptake of Nitrogen (FUN) model (Fisher *et al.* 2010; Brzostek *et al.* 2014b; Shi *et al.* 2016), running at daily resolution. See Appendix S1 in Supporting Information for a detailed description, equations, and parameters. FUN calculates N necessary to support plant growth using wood, root, and canopy biomass accrual and the C:N ratio of each plant tissue. Total C allocation to N acquisition is calculated as:

$$C_{acq} = N_{uptake} Cost_{acq} \quad (1)$$

where C_{acq} is total C allocated to N acquisition and $Cost_{acq}$ is the average C cost per unit N acquisition. Costs for root and mycorrhizal strategies depend inversely on root biomass (B_r) and soil inorganic N (N_{inorg}) (Brzostek *et al.* 2014b):

$$Cost_x = \frac{k_{N,x}}{N_{inorg}} + \frac{k_{C,x}}{B_r} \quad (2)$$

where x is an individual strategy and $k_{N,x}$ and $k_{C,x}$ are parameters that vary by mycorrhizal association. $Cost_{myco}$ in AM stands increases rapidly with decreases in N_{inorg}. Because ECM fungi can extract N directly from organic matter rather than relying on inorganic sources, $Cost_{myco}$ in ECM stands has a weaker dependence on N_{inorg} and a stronger dependence on B_r. Retranslocation only occurs during autumn leaf senescence, and its cost varies with leaf N. Symbiotic N fixation was negligible in our study sites. Total cost is calculated using a resistance framework analogy:

$$\frac{1}{Cost_{acq}} = \frac{1}{Cost_{root}} + \frac{1}{Cost_{retrans}} + \frac{1}{Cost_{myco}} \quad (3)$$

and C is allocated among strategies based on their relative costs:

$$C_x = \frac{C_{acq}}{Cost_x} \quad (4)$$

where C_x is carbon allocated to strategy x. C_{myco} and C_{root} are transferred to the soil model CORPSE, where their impacts on SOM cycling lead to a dynamic coupling between plants and soil (Figure 1).

2.2. Soil organic matter model

Soil C and N cycling were simulated using a modified version of the Carbon, Organisms, Rhizosphere, and Protection in the Soil Environment (CORPSE) model (Sulman *et al.* 2014), which simulates SOM decomposition with a focus on microbial activity and physical protection. For this study, we added N pools and transformations to CORPSE. See Appendix S1 for full equations, parameters, and details of the model. SOM is divided into three chemical types, representing resistant, labile and microbial necromass

compounds. Decomposition rates depend explicitly on microbial biomass along with temperature (T) and moisture (θ):

$$D_{C,i} = V_{max,i}(T) \cdot \left(\frac{\theta}{\theta_{sat}}\right)^3 \left(1 - \frac{\theta}{\theta_{sat}}\right)^{2.5} \cdot C_{U,i} \frac{C_M / C_{U,i}}{\frac{C_M}{C_{U,i}} + k_M} \quad (5)$$

$$D_{N,i} = V_{max,i}(T) \cdot \left(\frac{\theta}{\theta_{sat}}\right)^3 \left(1 - \frac{\theta}{\theta_{sat}}\right)^{2.5} \cdot N_{U,i} \frac{C_M / C_{U,i}}{\frac{C_M}{C_{U,i}} + k_M} \quad (6)$$

where D is the decomposition rate of organic C or N, $C_{U,i}$ and $N_{U,i}$ are unprotected C and N pools of type i, and C_M is microbial biomass C. Microbial biomass grows through SOM decomposition:

$$G_M = \begin{cases} \sum_i \left(\epsilon_{C,i} D_{C,i}\right) & , \Phi_N \geq -Imm_{max} \\ \mathrm{C{:}N}_M \cdot \left(\sum_i \left(\epsilon_{N,i} D_{N,i}\right) + Imm_{max}\right) + R_{maint} & , \Phi_N < -Imm_{max} \end{cases} \quad (7)$$

where G_M is microbial growth, $\epsilon_{C,i}$ and $\epsilon_{N,i}$ are C and N use efficiencies, R_{maint} is maintenance respiration, Imm_{max} is maximum N immobilization rate, $\mathrm{C{:}N}_M$ is microbial biomass C:N ratio, and Φ_N is net N balance of microbial growth, which determines immobilization or mineralization of N_{inorg}:

$$\Phi_N = \sum_i \left(\epsilon_{N,i} D_{N,i}\right) - \left(\sum_i \left(\epsilon_{C,i} D_{C,i}\right) - R_{maint}\right) / \mathrm{C{:}N}_M \quad (8)$$

Net N mineralization or immobilization during microbial SOM uptake is therefore determined by the C:N ratio of SOM taken up by microbes compared to microbial biomass C:N. If there is insufficient N to support microbial growth, excess C is converted to CO_2 as overflow respiration (Schimel & Weintraub 2003). N mineralization also occurs during decomposition and microbial biomass turnover. N_{inorg} is simulated as a single pool, without distinguishing between ammonium and nitrate, and nitrification is not simulated. Labile SOM, which has high ϵ_C and V_{max} values, drives priming effects by

promoting microbial growth and thereby accelerating decomposition. The model represents physically protected SOM as a separate set of pools that contains the same three chemical types of SOM and is inaccessible to microbial decomposition. SOM is converted from unprotected to protected forms at different fixed rates depending on chemical class, with microbial necromass having the fastest protection rate:

$$\frac{dC_{P,i}}{dt} = C_{U,i} \cdot \gamma_i - \frac{C_{P,i}}{\tau_P} \quad (8)$$

$$\frac{dN_{P,i}}{dt} = N_{U,i} \cdot \gamma_i - \frac{N_{P,i}}{\tau_P} \quad (9)$$

where $C_{P,i}$ and $N_{P,i}$ are protected C and N, respectively and γ_i and τ_P are parameters. Because litter with a higher labile content produces more microbial biomass and eventual necromass production, it drives faster protected C formation compared to slower-cycling litter.

Our model configuration divides organic matter pools among three compartments, representing the litter layer, rhizosphere, and bulk soil. Each compartment contains its own microbial biomass and SOM pools (although the litter layer does not contain protected SOM), allowing the model to simulate contrasts in microbial activity among compartments. Leaf litter is added to the litter layer, while root litter is divided between the rhizosphere and bulk soil based on rhizosphere size. C_{root} calculated by the FUN model is assumed to be equivalent to root exudation and added to the rhizosphere as labile C. C_{myco} is divided between the rhizosphere and bulk soil, reflecting the ability of mycorrhizal hyphae to forage outside the rhizosphere. These labile C subsidies stimulate microbial growth, increasing SOM decomposition rates but also increasing microbial N

demand. As a result, they can increase N mineralization or immobilization, depending on conditions.

2.3. Empirical input and validation data

We ran the model using data collected during the 2013 growing season across 45 forested plots that spanned a mycorrhizal gradient in southern Indiana, USA. The plots were located at one of three sites: Morgan Monroe State Forest (MMSF; 39º19.37'N, 86º24.8'W), Lilly Dickey Woods (LDW; 39º14.58'N, 86º12.58'W), and Griffey Woods (GW; 39º11.9'N, 86º30.76'W), each of which contains a diverse mixture of AM and ECM trees. Fifteen 12m x 12m plots were established at each site to cover a range in basal area fraction from 100% AM dominated to 100% ECM dominated (Table S3). Dominant ECM trees included American beech (*Fagus grandifolia* Ehrh.), northern red oak (*Quercus rubra* L.), white oak (*Quercus alba* L.), black oak (*Quercus velutina* Lam.), and various hickories (*Carya spp.*). Dominant AM trees included sugar maple (*Acer saccharum* Marsh.), tulip poplar (*Liriodendron tulipifera* L.), white ash (*Fraxinus Americana* L.), black walnut (*Juglans nigra* L.), black cherry (*Prunus serotina* Ehrh.) and sassafras (*Sassafras albidum* Nutt.) (Cheeke *et al.* 2017). All three sites are located within approximately 40km of each other and have similar climate and topography. However, stand age of LDW is more than 150 years while stand ages of MMSF and GW are approximately 80-90 years.

We measured annual wood production in each plot using dendrometer bands applied to every tree greater than 10cm diameter at breast height (DBH). Annual changes in

247 diameter were converted to biomass increments using allometric equations (Brzostek *et*
248 *al.* 2014a). Leaf litter was collected in each plot, separated by species into ECM and AM
249 fractions, dried, weighed, and analyzed for %C and %N. Leaf area index (LAI) in each
250 plot was measured at the peak of the growing season using a LAI-2000 system (LI-COR
251 Inc., Lincoln, NE, USA). Canopy leaf %N was measured using foliar samples collected
252 from the top of the canopy and multiplied by LAI to estimate total foliar N on a g m^{-2}
253 basis. %C and %N of wood were estimated using samples from a nearby site at Moore's
254 Creek, IN for the eight most common tree species. All %C and %N analyses were made
255 using a CN elemental analyzer on oven-dried samples (Costech Analytical, Valencia, CA,
256 USA).
257
258 Soils were sampled to a depth of 15 cm four times during the 2013 growing season (May,
259 June, August, October). Fine roots (less than 2mm in diameter) were picked from each
260 soil sample, weighed, and analyzed for %C and %N in the same manner as aboveground
261 tissues. We assumed a one-year fine root turnover time for both AM and ECM trees
262 (McCormack *et al.* 2014). Consequently, annual fine root production equaled mean root
263 biomass over the four sampling dates. Soil N mineralization was measured using three-
264 week aerobic lab incubations that measured the increase in NH_4^+ and NO_3^- in incubated
265 samples vs. an initial sample. We used previously published measurements of root
266 exudation from AM and ECM roots at GW (Yin *et al.* 2014) and morphology data for
267 AM and ECM temperate tree species (Comas & Eissenstat 2009; McCormack *et al.*
268 2014) to estimate root exudation rates for each plot. We multiplied the mean exudation
269 rate for each mycorrhizal association (mg C g fine $root^{-1}$ day^{-1}) by total AM or ECM fine

root length in each plot. We assumed that exudation occurred only during the period when the canopy remained green. The root morphology and biomass measurements were also used to estimate the size of the rhizosphere for each plot, assuming that roots are cylindrical and that the rhizosphere extends 1mm from the root surface (Meier *et al.* 2014; Finzi *et al.* 2015). Measurements of C and N mineralization in the rhizosphere compared to bulk soil from Yin *et al.* (2014) were used for comparison with simulations.

Annual data were converted to daily estimates for driving model simulations using phenological data previously collected at MMSF. Weekly LAI and greenness data from MMSF were used to control the timing of C allocation to leaves as well as the timing of litter fall (Dragoni *et al.* 2011). Wood production phenology was derived from weekly measurements of DBH at MMSF (Brzostek *et al.* 2014a). Root phenology was estimated using weekly measurements of root biomass at MMSF during the 2005 growing season (CA Wayson, unpublished data). Each phenological time series was fit with a 2^{nd} order polynomial using the curve-fitting tool in Matlab and normalized between zero and one. We then multiplied the annual biomass growth for each component (roots, leaves, and wood) by the first derivative of its phenological time series to calculate daily changes.

2.4. Model calibration, validation, and experimental setup

Along with the daily plant C and N time series described above, we drove the model using observed soil temperature and moisture from the MMSF Ameriflux tower from 2013. Simulations received atmospheric deposition at a constant rate of 6 kg N ha^{-1} $year^{-1}$

293 based on typical rates observed in the region. Model parameters were based on previously
294 published values where possible (Brzostek *et al.* 2014b; Sulman *et al.* 2014). Some
295 recalibration of parameters relative to previously published values was required because
296 explicitly simulating the soil N cycle changed decomposition rates and N availability
297 relative to previously published FUN and CORPSE simulations. Parameters were
298 adjusted to match observed mean SOM stocks and N mineralization rates. Simulations
299 were initialized by running the model with looped meteorology and litter inputs until soil
300 pools reached approximate steady state.
301
302 Plots were divided into AM and ECM components using the relative basal areas of AM
303 and ECM trees in each plot, with tissue C:N for each mycorrhizal association based on
304 site measurements. Based on known differences in litter qualities, AM litter had a higher
305 initial labile C fraction (30%) than ECM litter (10%). Leaf litter C:N ratios were
306 determined by the FUN model using simulated retranslocation.
307
308 Experimental simulations included the following: (1) control simulations, in which model
309 parameters reflected the spinup conditions; (2) reversed mycorrhizal association
310 simulations, in which plant and microbial C:N ratios, FUN cost parameters, and litter
311 decomposition properties were reversed to simulate vegetation growing on soil that had
312 developed under the opposite mycorrhizal association; and (3) elevated productivity
313 simulations, in which plant N demand and litter production were increased by 20%. Each
314 set of simulations included one version in which C_{root} and C_{myco} were added to the soil,
315 and one in which these transfers were ignored. This allowed us to directly assess the

316 impacts of microbial subsidies on SOM cycling and N mineralization. Note that because
317 NPP was prescribed based on measurements, litter production was not limited by N
318 availability. To separate the effects of coupled plant-microbial interactions from
319 increased litter inputs, different versions of the elevated productivity simulations were
320 conducted in which C_{root} and C_{myco} were either prescribed using values from the control
321 simulation or increased as calculated by the FUN model based on the increased N
322 demand. Elevated productivity simulations were integrated for seven years and then
323 averaged over the next two years for comparison with control simulations.

324 3. Results

325 3.1. Model performance relative to observations

326

327 The model accurately reproduced variations in root exudation across the mycorrhizal
328 gradient, although it slightly overestimated the flux in AM-dominant plots and
329 underestimated it in ECM-dominant plots (Fig. 2a). Exudation increased with increasing
330 plot ECM fraction, from 12 gC m^{-2} $year^{-1}$ in AM-dominant plots to near 30 gC m^{-2} $year^{-1}$
331 in ECM-dominant plots. Root exudation stimulated C and N mineralization in the
332 rhizosphere via increases in microbial biomass growth and turnover (Figure 2b). The
333 modeled responses were somewhat smaller in magnitude than the observed responses, but
334 the general pattern matched observations, with ECM-dominant plots experiencing
335 stronger rhizosphere stimulation of both C and N mineralization than AM-dominant
336 plots. In addition, modeled and observed values had similar ratios between C and N
337 mineralization (Figure 2b).

SOM stocks and N cycling varied strongly across the mycorrhizal gradient (Figure 3). N mineralization (Fig. 3g), protected soil C and N (Fig. 3c,f), soil C turnover (Fig. 3h), and microbial biomass (Fig. 3i) all decreased across the gradient from AM to ECM dominance. By contrast, greater ECM dominance drove increases in unprotected C and N (Fig. 3b,e). Total C was higher in ECM plots (Fig. 3a) while total N was higher in AM plots (Fig. 3d), reflecting the low C:N ratio of protected SOM and the high proportion of total N stored in protected pools. We quantified the impact of microbial subsidies by conducting paired simulations where FUN-determined rhizosphere C transfers were either added to soil or ignored. These simulations were compared after being integrated for four years. Microbial subsidies reduced total soil C and N stocks, with the greatest losses occurring in ECM-dominant plots (Fig. 3a,d). These reductions were driven by losses of unprotected SOM, which were greatest in ECM-dominant plots (Fig. 3b). Microbial subsidies slightly increased protected C and N stocks. However, changes in protected SOM were small compared to changes in unprotected SOM. Microbial subsidies increased N mineralization rates across the gradient (Fig. 3g), with the strongest effects occurring in ECM-dominant plots. The increases in N mineralization were matched by increases in C turnover rate (Fig. 3h) driven by enhanced microbial biomass (Fig. 3i).

Because microbial subsidies accelerated both C and N mineralization, increases in N availability were accompanied by losses of SOC. The ratio of SOC loss to N

mineralization varied across the gradient from 14 gC gN^{-1} in AM-dominant plots to 28 gC gN^{-1} in ECM-dominant plots (Figure 4).

3.2. Responses to change in dominant mycorrhizal associations

To assess couplings between vegetation and soils, we reversed mycorrhizal associations across the gradient and simulated how soils changed over time (Figure 5). Unprotected C and N stocks moved relatively quickly toward the values associated with the newly dominant vegetation, although AM soils with ECM vegetation had lower stocks than unmodified ECM plots after 50 years (Fig. 5b,e). By contrast, protected C and N stocks changed more slowly (Fig. 5c,f). Total C stocks overshot unmodified values, with AM soils colonized by ECM vegetation eventually accumulating more C than ECM soils with matched vegetation and stocks in ECM soils colonized by AM vegetation declining below those of AM soils with matched vegetation (Fig. 5a). Total N changed only slightly, with stocks in ECM soils colonized by AM vegetation slightly increasing relative to those of ECM soils with matching vegetation, and stocks in AM soils colonized by ECM vegetation slightly declining relative to AM soils with matching vegetation (Fig. 5d). N mineralization changed rapidly, temporarily overshooting the values associated with the dominant vegetation on matched soils (Fig. 5g). Soil C turnover rate and microbial biomass changed rapidly in the first year and then evolved more slowly over ensuing years (Fig. 5h,i).

3.3. Response to increased vegetation productivity

We modeled the impacts of increasing ecosystem productivity by conducting simulations in which litter production, root turnover, and vegetation N demand were increased by 20% (Figure 6). This increased rhizosphere C allocation by approximately 14% in AM-dominant plots and 19% in ECM-dominant plots (Fig. 6a,d). These increased microbial subsidies stimulated N mineralization, with stronger effects occurring in ECM-dominant plots. However, the N mineralization response was relatively flat with respect to stand composition when ECM fraction was greater than approximately 40% (Fig 6b). Higher microbial subsidies also stimulated SOM decomposition, depleting soil C relative to simulations without increases in microbial subsidies. This effect was greater in ECM-dominant plots than in AM-dominant plots (Fig. 6c,f).

4. Discussion

By integrating new theoretical understanding with empirical measurements of the processes that couple SOM to vegetation function, FUN-CORPSE represents a significant advancement from current TBM model structures. Most existing model frameworks represent plants and soils as distinct processes connected only by indirect feedbacks related to litter inputs and soil N mineralization (e.g Zaehle *et al.* 2014). Here, we show that by dynamically linking rhizosphere C allocation to soil microbial growth and SOM cycling (Fig. 1), FUN-CORPSE accurately captures empirical differences between AM- and ECM-dominant plots (Figs. 2, 3), illuminates the extent to which plant

404 influences on soil properties persist over time (Fig. 5), and provides a framework for
405 estimating the impacts of priming effects on ecosystem C balance (Figs. 4, 6).
406 Collectively, these results suggest that TBM simulations of temperate forests could be
407 improved by explicitly coupling plants with soil microbial dynamics and physical
408 protection processes.
409
410 A key strength of our simulations lies in the use of detailed plot-level data to
411 parameterize, force, and validate the model. FUN-CORPSE captured the greater observed
412 root exudation rates in ECM compared to AM rhizospheres (Fig. 2a), which drove greater
413 stimulation of rhizosphere C and N mineralization that was consistent with observations
414 (Fig. 2b). However, rhizosphere stimulation in model simulations was generally lower
415 than in observations. This underestimation could be due to uncertainty in laboratory-
416 based C and N mineralization measurements but may also reflect uncertainty in model
417 parameters and processes. Roots in the model are unable to forage into new unexploited
418 patches, a key priority for future model development (Cheng *et al.* 2014; Chen *et al.*
419 2016). There are also considerable uncertainties in our parameterization of microbial
420 traits (e.g., CUE, turnover rates, and stoichiometry). These uncertainties are not unique to
421 FUN-CORPSE, but reflect a critical need across recent microbial decomposition models
422 for more empirical data on how microbial traits vary across environmental gradients
423 (including gradients in mycorrhizal association). In addition, the model slightly
424 underestimated the difference in root exudation between AM-dominant and ECM-
425 dominant stands at the ends of the mycorrhizal gradient (Fig. 2a). As a result, the
426 differences in C and N pools and mycorrhizal effects across the gradient could have been

427 slightly underestimated. Finally, FUN-CORPSE is designed to predict plant-microbial
428 interactions in the upper soil layers (0-30cm). Thus, the model does not capture dynamics
429 in deeper soil layers, where greater physically protected SOM stocks in AM soils could
430 potentially outweigh the greater total soil C storage we predict in ECM soils.
431
432 FUN-CORPSE predicted substantial differences in soil C and N stocks and their
433 responses to microbial subsidies between AM and ECM ecosystems. These differences
434 emerged from the model structure, which integrates current theoretical and empirical
435 evidence that mineral sorption and aggregation processes preferentially protect organic
436 compounds derived from microbial extracellular enzyme production and biomass
437 turnover (Cotrufo *et al.* 2013; Bingham & Cotrufo 2016). In AM plots, the lower C:N
438 ratio and higher labile content of litter drove faster decomposition and higher microbial
439 biomass production leading to the majority of SOM being physically protected (Fig.
440 3b,c). By contrast, the more chemically resistant ECM litter produced slower
441 decomposition and lower microbial biomass production, reducing the physically
442 protected proportion of SOM. The higher proportion of unprotected SOM in ECM plots
443 meant greater vulnerability to priming effects, so that rhizosphere C allocation
444 accelerated SOM turnover to a greater degree in ECM soils than in AM soils (Fig. 3).
445 Thus, the model suggests that differences in SOM properties and the strength of priming
446 effects between AM and ECM stands are due to interactions between litter chemistry and
447 the formation of physically protected SOM. These simulations assumed that soil
448 mineralogical properties did not vary between AM and ECM stands. For sites occurring
449 on different soils, variations in mineralogical factors such as clay content or reactive

450 mineral surface area could outweigh the effects of litter properties. Further investigation
451 into the relative effects of these litter and mineralogical factors could help refine our
452 understanding of these processes.
453
454 Simulations with reversed mycorrhizal associations revealed important ecological
455 processes at multiple time scales (Figure 5). AM vegetation growing on ECM soils had
456 lower rates of N mineralization than unmodified AM plots for the first few years until
457 litter deposition provided new N sources. This suggests that slower N cycling in ECM
458 stands could pose challenges for initial growth of AM vegetation by restricting N
459 availability for nitrophilic AM plants. This is consistent with the persistence of mono-
460 dominant ECM forest stands in both temperate and tropical regions (e.g. Frelich *et al.*
461 1993; McGuire 2008). Over longer time scales, the stability of physically protected SOM
462 pools led to long-lasting differences in C stocks. Growth of ECM vegetation on
463 historically AM soils enhanced C stocks, while growth of AM vegetation on ECM soils
464 depleted soil C because a larger proportion was unprotected. Furthermore, N
465 mineralization was sensitive to soil history even after 50 years of changed mycorrhizal
466 associations. These results suggest that soil legacies of dominant plant communities could
467 drive long-term differences in ecosystem productivity and soil C storage. These results
468 are consistent with recent theoretical arguments that decomposition-prone litter can
469 enhance long-term SOM storage (Cotrufo *et al.* 2013) and contrast with suggestions that
470 soil C and N storage are independent of litter properties (Averill 2016).
471

FUN-CORPSE predicts that some forest ecosystems could sustain growth under elevated CO_2 by enhancing N mineralization through priming effects (Figure 6). This response varied with mycorrhizal association: ECM-dominant plots accelerated N mineralization to a greater degree than AM-dominant plots. This result is consistent with observations from elevated CO_2 experiments (Norby *et al.* 2010; Drake *et al.* 2011; Terrer *et al.* 2016). Current TBMs generally assume either that plant growth is not N limited (by omitting the N cycle) or that plant N availability is determined by soil decomposition processes that cannot be accelerated by plant C expenditures. Our results suggest an intermediate response: Increased NPP could accelerate N uptake beyond the rates supported by current soil N mineralization if plants stimulated SOM turnover via increased rhizosphere C expenditures. However, these increases in N mineralization may not be sufficient to fully support accelerated growth. The additional C cost incurred to fuel enhanced N uptake (Brzostek *et al.* 2014b) would also reduce plant production below the levels predicted in the absence of N limitation.

Whether priming increases or decreases ecosystem C storage depends on the balance between soil C losses due to accelerated decomposition and vegetation C gains facilitated by increased N mineralization (Figures 4 and 6). Our results suggest that this net balance varies with mycorrhizal association, with ECM ecosystems losing more SOC per unit N mineralization than AM ecosystems. This effect was driven by two factors. First, the higher C:N ratios of litter and SOM in ECM stands meant that more C had to be decomposed per unit of N released. Second, the larger magnitude of rhizosphere C allocation in ECM stands drove higher N immobilization. Using the FUN-CORPSE

framework, we can estimate the critical C:N ratio of plant biomass accumulation at which net ecosystem C flux would shift from a net loss to a net gain if all liberated N were used to build biomass. Based on our simulations, this ratio has a lower limit of approximately 14 for AM stands and 28 for ECM stands. This relationship was consistent with Midgley et al (2016), who observed a two-fold difference in the ratio of C mineralization to N mineralization between AM and ECM plots. If the majority of additional plant growth went to woody tissue with a typical C:N ratio of 300 or more, priming effects would likely drive a net increase in total ecosystem C storage, although tree mortality or depletion of soil N over time could eventually limit this increase.

Our coupled plant-soil model FUN-CORPSE connects plant investment of C toward N acquisition with the resulting impacts on soil microbial activity and SOM cycling. Our results suggest that microbial subsidies can accelerate SOM mineralization, liberating N to support plant growth at the expense of soil C losses. However, the capacity to stimulate N availability varies with mycorrhizal association, with ECM-dominant forests having a higher capacity than AM-dominant forests. Differences in rhizosphere C allocation and litter properties between mycorrhizal associations also drive differences in SOM properties that persist over long time periods. While simulating mycorrhizal associations as separate plant functional types in TBMs presents parameterization difficulties, emerging methods based on remote sensing (Fisher *et al.* 2016) or trait-based approaches (van Bodegom *et al.* 2014) show promise for generating global estimates of distributions of mycorrhizal associations and their traits. Thus, it is becoming increasingly feasible to integrate mycorrhizal associations as controls on plant-microbial

518 interactions into earth system models, thereby addressing the critical omission of plant-
519 soil coupling in responses to global change (Warren *et al.* 2015; Brzostek *et al.* 2016;
520 Terrer *et al.* 2016).
521
522
523 **Acknowledgments:** This material is based upon work supported by the U.S. Department
524 of Energy Office of Biological and Environmental Research, Terrestrial Ecosystem
525 Science Program (DE-SC0016188), and the US National Science Foundation Ecosystem
526 Studies Program (grant #1153401). The field research was conducted at Indiana
527 University's Research and Teaching Preserve. Thanks to Z. Brown, T. Roman, and L.
528 Jacobs for field and data processing help. Thanks to Dr. C. Chou, Dr. A. Porporato, and
529 two anonymous reviewers for helpful comments on the manuscript. This report was
530 prepared by B. Sulman under award NA14OAR4320106 from the National Oceanic and
531 Atmospheric Administration, U.S. Department of Commerce. This study was also
532 supported by NOAA Climate Program Office's Atmospheric Chemistry, Carbon Cycle,
533 and Climate program, award #NA15OAR4310065. The statements, findings,
534 conclusions, and recommendations are those of the author(s) and do not necessarily
535 reflect the views of the National Oceanic and Atmospheric Administration or the U.S.
536 Department of Commerce.
537
538 **References:**
539
540
541 Averill, C. (2016). Slowed decomposition in ectomycorrhizal ecosystems is independent
542 of plant chemistry. *Soil Biology and Biochemistry*, 102, 52-54.

Averill, C., Turner, B.L. & Finzi, A.C. (2014). Mycorrhiza-mediated competition between plants and decomposers drives soil carbon storage. *Nature*, 505, 543-545.

Bingham, A.H. & Cotrufo, M.F. (2016). Organic nitrogen storage in mineral soil: Implications for policy and management. *Science of the Total Environment*, 551, 116-126.

Brzostek, E.R., Dragoni, D., Schmid, H.P., Rahman, A.F., Sims, D., Wayson, C.A. *et al.* (2014a). Chronic water stress reduces tree growth and the carbon sink of deciduous hardwood forests. *Global Change Biol*, 20, 2531-2539.

Brzostek, E.R., Fisher, J.B. & Phillips, R.P. (2014b). Modeling the carbon cost of plant nitrogen acquisition: Mycorrhizal trade-offs and multipath resistance uptake improve predictions of retranslocation. *Journal of Geophysical Research-Biogeosciences*, 119, 1684-1697.

Brzostek, E.R., Rebel, K.T., Smith, K.R. & Phillips, R.P. (2016). Integrating mycorrhizae into global scale models: a journey toward relevance in the earth's climate system. In: *Mycorrhizal mediation of soil: fertility, structure, and carbon storage* (eds. Johnson, NC, Gehring, C & Jansa, J). Elsevier Amsterdam, The Netherlands.

Cheeke, T.E., Phillips, R.P., Brzostek, E.R., Rosling, A., Bever, J.D. & Fransson, P. (2017). Dominant mycorrhizal association of trees alters carbon and nutrient cycling by selecting for microbial groups with distinct enzyme function. *New Phytol*, 214, 432-442.

Chen, W., Koide, R.T., Adams, T.S., Deforest, J.L., Cheng, L. & Eissenstat, D.M. (2016). Root morphology and mycorrhizal symbioses together shape nutrient foraging strategies of temperate trees. *Proc. Nat. Acad. Sci. USA*, 113, 8741-8746.

Cheng, W., Parton, W.J., Gonzalez-Meler, M.A., Phillips, R., Asao, S., McNickle, G.G. *et al.* (2014). Synthesis and modeling perspectives of rhizosphere priming. *New Phytol*, 201, 31-44.

Comas, L.H. & Eissenstat, D.M. (2009). Patterns in root trait variation among 25 co-existing North American forest species. *New Phytol*, 182, 919-928.

Cornelissen, J., Aerts, R., Cerabolini, B., Werger, M. & van der Heijden, M. (2001). Carbon cycling traits of plant species are linked with mycorrhizal strategy. *Oecologia*, 129, 611-619.

Cotrufo, M.F., Wallenstein, M.D., Boot, C.M., Denef, K. & Paul, E.A. (2013). The Microbial Efficiency-Matrix Stabilization (MEMS) framework integrates plant litter decomposition with soil organic matter stabilization: Do labile plant inputs form stable soil organic matter? *Global Change Biol*, 19, 988-995.

Dragoni, D., Schmid, H.P., Wayson, C.A., Potter, H., Grimmond, C.S.B. & Randolph, J.C. (2011). Evidence of increased net ecosystem productivity associated with a longer vegetated season in a deciduous forest in south-central Indiana, USA. *Global Change Biol*, 17, 886-897.

Drake, J.E., Gallet-Budynek, A., Hofmockel, K.S., Bernhardt, E.S., Billings, S.A., Jackson, R.B. *et al.* (2011). Increases in the flux of carbon belowground stimulate nitrogen uptake and sustain the long-term enhancement of forest productivity under elevated CO_2. *Ecology Letters*, 14, 349-357.

Finzi, A.C., Abramoff, R.Z., Spiller, K.S., Brzostek, E.R., Darby, B.A., Kramer, M.A. *et al.* (2015). Rhizosphere processes are quantitatively important components of terrestrial carbon and nutrient cycles. *Global Change Biol*, 21, 2082-2094.

589 Finzi, A.C., Norby, R.J., Calfapietra, C., Gallet-Budynek, A., Gielen, B., Holmes, W.E. *et*
590 *al.* (2007). Increases in nitrogen uptake rather than nitrogen-use efficiency support
591 higher rates of temperate forest productivity under elevated CO_2. *Proc. Nat. Acad.*
592 *Sci. USA*, 104, 14014-14019.
593 Fisher, J.B., Sitch, S., Malhi, Y., Fisher, R.A., Huntingford, C. & Tan, S.Y. (2010).
594 Carbon cost of plant nitrogen acquisition: A mechanistic, globally applicable
595 model of plant nitrogen uptake, retranslocation, and fixation. *Global Biogeochem.*
596 *Cycles*, 24, GB1014.
597 Fisher, J.B., Sweeney, S., Brzostek, E.R., Evans, T.P., Johnson, D.J., Myers, J.A. *et al.*
598 (2016). Tree-mycorrhizal associations detected remotely from canopy spectral
599 properties. *Global Change Biol*, 22, 2596-2607.
600 Frelich, L.E., Calcote, R.R., Davis, M.B. & Pastor, J. (1993). Patch Formation and
601 Maintenance in an Old-Growth Hemlock-Hardwood Forest. *Ecology*, 74, 513-
602 527.
603 Friedlingstein, P., Cox, P., Betts, R., Bopp, L., von Bloh, W., Brovkin, V. *et al.* (2006).
604 Climate–Carbon Cycle Feedback Analysis: Results from the C4MIP Model
605 Intercomparison. *Journal of Climate*, 19, 3337-3353.
606 Heimann, M. & Reichstein, M. (2008). Terrestrial ecosystem carbon dynamics and
607 climate feedbacks. *Nature*, 451, 289-292.
608 Hungate, B.A., Dukes, J.S., Shaw, M.R., Luo, Y. & Field, C.B. (2003). Nitrogen and
609 climate change. *Science*, 302, 1512.
610 Kuzyakov, Y. (2010). Priming effects: Interactions between living and dead organic
611 matter. *Soil Biology and Biochemistry*, 42, 1363-1371.
612 Lin, G., McCormack, M.L., Ma, C. & Guo, D. (2016). Similar below-ground carbon
613 cycling dynamics but contrasting modes of nitrogen cycling between arbuscular
614 mycorrhizal and ectomycorrhizal forests. *New Phytol*, 213, 1440-1451.
615 McCormack, M.L., Adams, T.S., Smithwick, E.A.H. & Eissenstat, D.M. (2014).
616 Variability in root production, phenology, and turnover rate among 12 temperate
617 tree species. *Ecology*, 95, 2224-2235.
618 McGuire, K.L. (2008). Ectomycorrhizal Associations Function to Maintain Tropical
619 Monodominance. In: *Mycorrhizae: Sustainable Agriculture and Forestry* (ed.
620 Siddiqui, ZA). Springer Science + Business Media B.V., pp. 287-302.
621 Meier, I.C., Pritchard, S.G., Brzostek, E.R., McCormack, M.L. & Phillips, R.P. (2014).
622 The rhizosphere and hyphosphere differ in their impacts on carbon and nitrogen
623 cycling in forests exposed to elevated CO_2. *New Phytol*, 205, 1164-1174.
624 Midgley, M.G., Brzostek, E. & Phillips, R.P. (2015). Decay rates of leaf litters from
625 arbuscular mycorrhizal trees are more sensitive to soil effects than litters from
626 ectomycorrhizal trees. *Journal of Ecology*, 103, 1454-1463.
627 Midgley, M. G., & Phillips, R. P. (2016). Resource stoichiometry and the biogeochemical
628 consequences of nitrogen deposition in a mixed deciduous forest. *Ecology*,
629 *97*(12), 3369–3378, doi:10.1002/ecy.1595.
630 Norby, R.J., Warren, J.M., Iversen, C.M., Medlyn, B.E. & McMurtrie, R.E. (2010). CO_2
631 enhancement of forest productivity constrained by limited nitrogen availability.
632 *Proc. Nat. Acad. Sci. USA*, 107, 19368-19373.

633 Pellitier, P. T., & Zak, D. R. (2017). Ectomycorrhizal fungi and the enzymatic liberation
634 of nitrogen from soil organic matter: why evolutionary history matters. *New*
635 *Phytologist*, *103*, 495–6, doi:10.1111/nph.14598.
636 Phillips, R.P., Brzostek, E. & Midgley, M.G. (2013). The mycorrhizal-associated nutrient
637 economy: a new framework for predicting carbon-nutrient couplings in temperate
638 forests. *New Phytol*, 199, 41-51.
639 Phillips, R.P., Finzi, A.C. & Bernhardt, E.S. (2011). Enhanced root exudation induces
640 microbial feedbacks to N cycling in a pine forest under long-term CO_2
641 fumigation. *Ecology Letters*, 14, 187-194.
642 Phillips, R.P., Meier, I.C., Bernhardt, E.S., Grandy, A.S., Wickings, K. & Finzi, A.C.
643 (2012). Roots and fungi accelerate carbon and nitrogen cycling in forests exposed
644 to elevated CO_2. *Ecology Letters*, 15, 1042-1049.
645 Read, D.J. & Perez Moreno, J. (2003). Mycorrhizas and nutrient cycling in ecosystems –
646 a journey towards relevance? *New Phytol*, 157, 475-492.
647 Schimel, J.P. & Weintraub, M.N. (2003). The implications of exoenzyme activity on
648 microbial carbon and nitrogen limitation in soil: a theoretical model. *Soil Biology*
649 *and Biochemistry*, 35, 549-563.
650 Shi, M., Fisher, J.B., Brzostek, E.R. & Phillips, R.P. (2016). Carbon cost of plant
651 nitrogen acquisition: global carbon cycle impact from an improved plant nitrogen
652 cycle in the Community Land Model. *Global Change Biol*, 22, 1299-1314.
653 Sulman, B.N., Phillips, R.P., Oishi, A.C., Shevliakova, E. & Pacala, S.W. (2014).
654 Microbe-driven turnover offsets mineral-mediated storage of soil carbon under
655 elevated CO_2. *Nature Climate change*, 4, 1099-1102.
656 Terrer, C., Vicca, S., Hungate, B.A., Phillips, R.P. & Prentice, I.C. (2016). Mycorrhizal
657 association as a primary control of the CO_2 fertilization effect. *Science*, 353, 72-
658 74.
659 Thomas, R.Q., Brookshire, E.N.J. & Gerber, S. (2015). Nitrogen limitation on land: how
660 can it occur in Earth system models? *Global Change Biol*, 21, 1777-1793.
661 van Bodegom, P.M., Douma, J.C. & Verheijen, L.M. (2014). A fully traits-based
662 approach to modeling global vegetation distribution. *Proceedings of the National*
663 *Academy of Sciences*, 111, 13733-13738.
664 Warren, J.M., Hanson, P.J., Iversen, C.M., Kumar, J., Walker, A.P. & Wullschleger, S.D.
665 (2015). Root structural and functional dynamics in terrestrial biosphere models –
666 evaluation and recommendations. *New Phytol*, 205, 59-78.
667 Wieder, W.R., Cleveland, C.C., Smith, W.K. & Todd-Brown, K. (2015). Future
668 productivity and carbon storage limited by terrestrial nutrient availability. *Nature*
669 *Geoscience*, 8, 441-444.
670 Yin, H., Wheeler, E. & Phillips, R.P. (2014). Root-induced changes in nutrient cycling in
671 forests depend on exudation rates. *Soil Biology and Biochemistry*, 78, 213-221.
672 Zaehle, S., Medlyn, B.E., De Kauwe, M.G., Walker, A.P., Dietze, M.C., Hickler, T. *et al.*
673 (2014). Evaluation of 11 terrestrial carbon-nitrogen cycle models against
674 observations from two temperate Free-Air CO2 Enrichment studies. *New Phytol*,
675 202, 803-822.
676

677

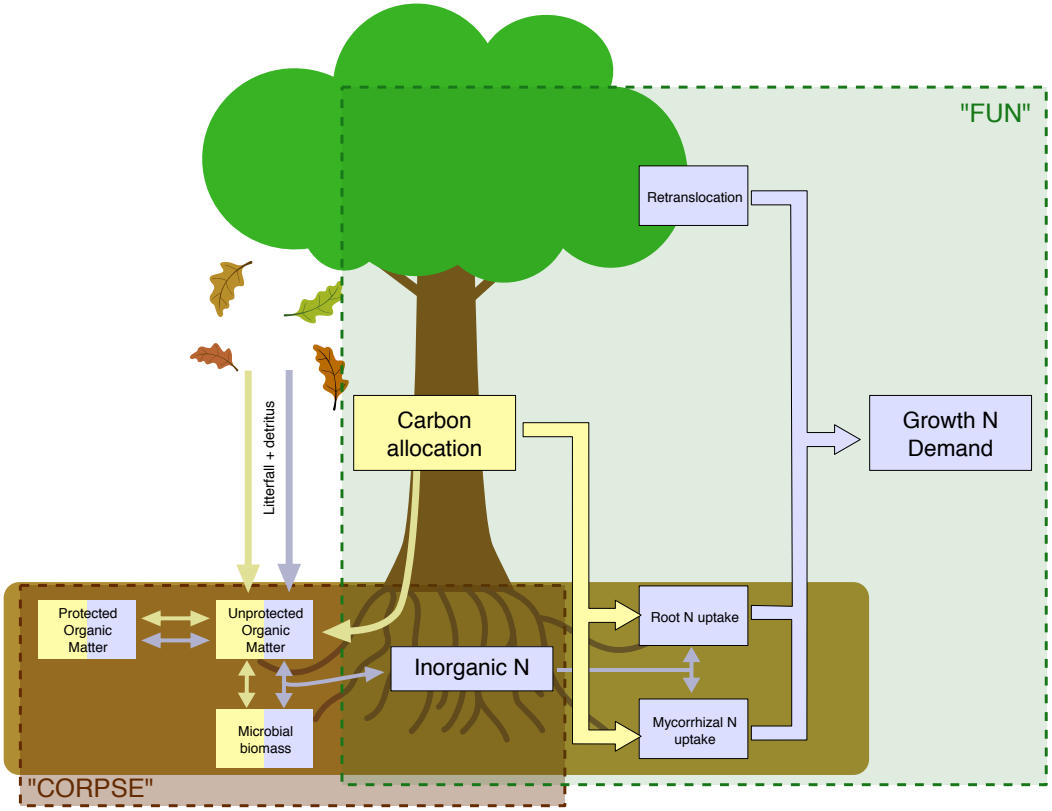

Figure 1: Diagram of FUN-CORPSE model. Carbon and nitrogen stocks and flows are color-coded, with carbon in yellow and nitrogen in purple. Different compartments (litter layer, rhizosphere, and bulk soil) are not shown.

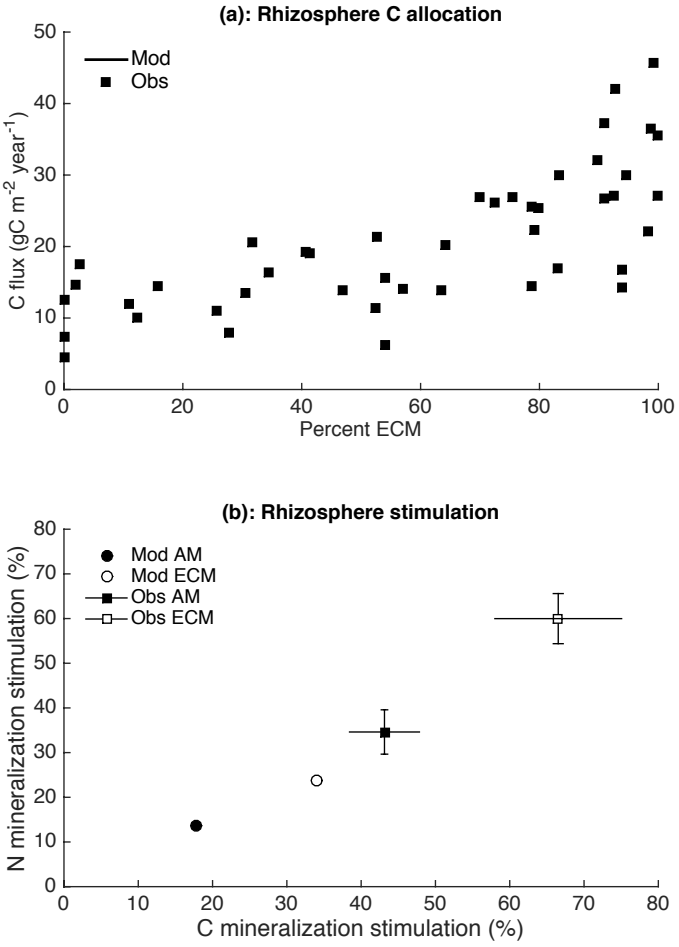

683

684

685 Figure 2: FUN-CORPSE captures differences between mycorrhizal associations in the
686 amount of C transferred to the rhizosphere and its impacts on soil dynamics. (a):
687 Modeled vs. observed C allocation to the rhizosphere. (b): Modeled vs. observed
688 rhizosphere stimulation C and N mineralization rates. Values are percent differences
689 between the rhizosphere and bulk soil, where positive values are an enhancement in the
690 rhizosphere. Observed data are derived from Yin et al. (2015).

691

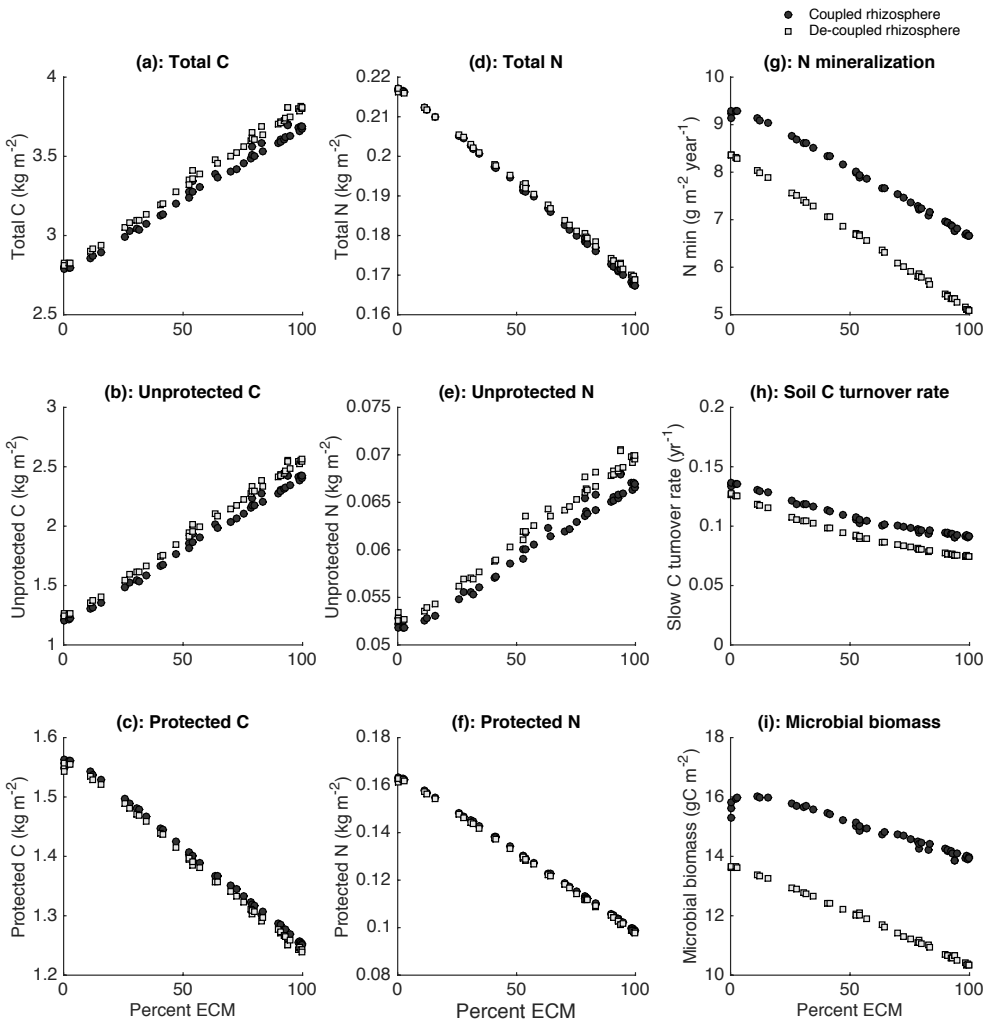

692
693 Figure 3: The impact of C transfers to the rhizosphere on soil dynamics after five years.
694 (a) Total soil C, (b) Unprotected soil C, (c) Protected soil C, (d) total soil N, (e)
695 unprotected soil N, (f) protected soil N, (g) N mineralization rate, (h) Turnover rate of
696 slow, unprotected soil C pool and (f) microbial biomass as a function of mycorrhizal
697 association. Lighter symbols show simulations with no rhizosphere C deposition.

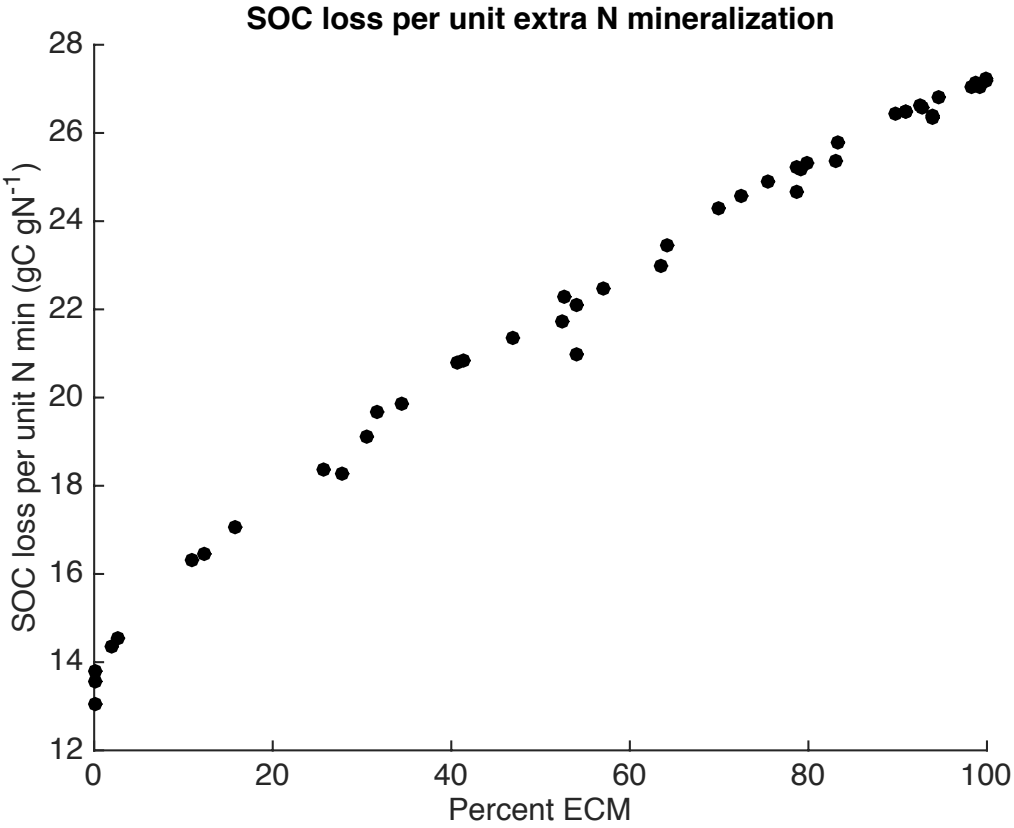

Figure 4: The amount of SOC loss due to accelerated decomposition per unit of accelerated N mineralization.

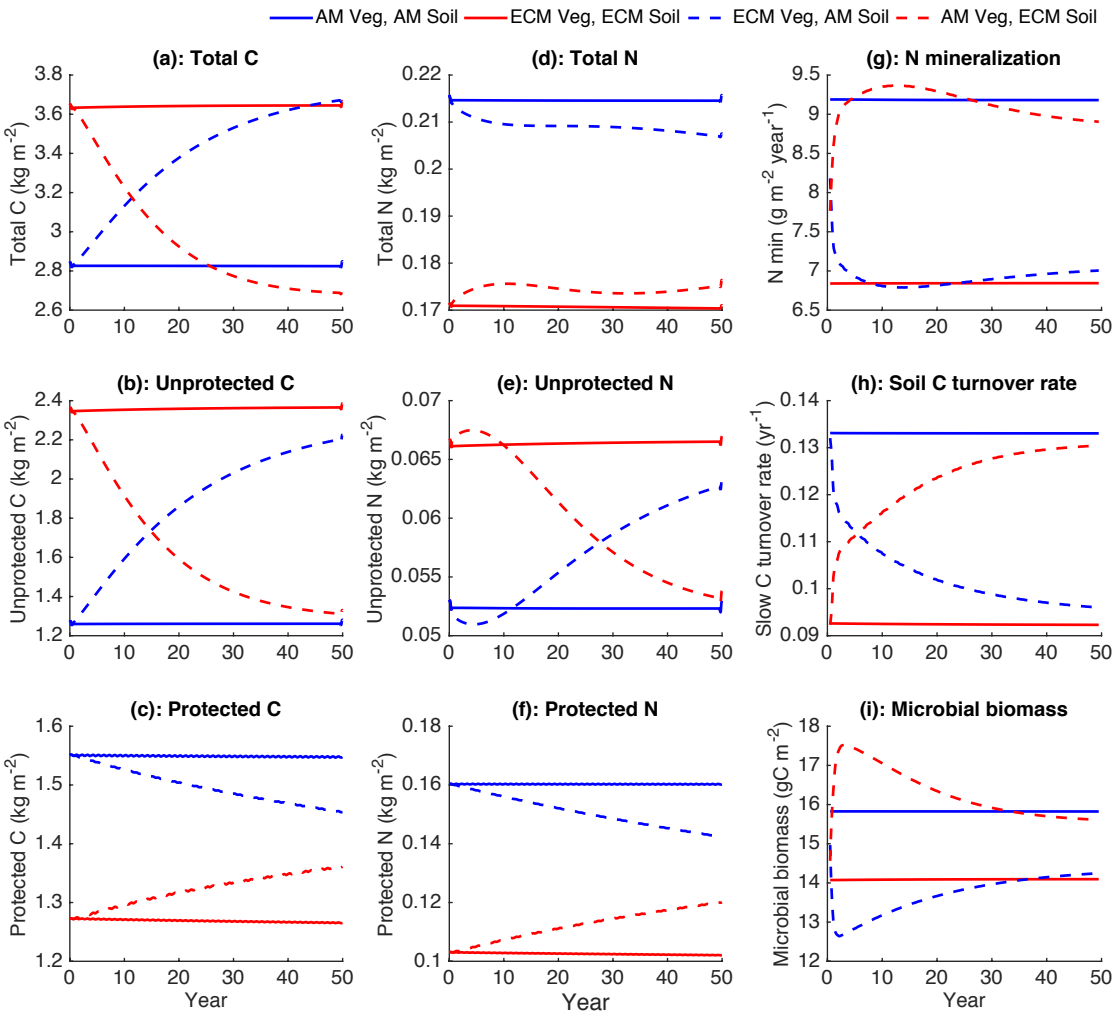

701

702 Figure 5: Reversing mycorrhizal associations drives changes in soil C and N cycling over

703 time. Red lines show soils with ECM-dominant history and blue lines show soils with

704 AM-dominant history. Solid lines have vegetation matched to prior soil history, and

705 dashed lines have reversed plant mycorrhizal associations relative to soil history.

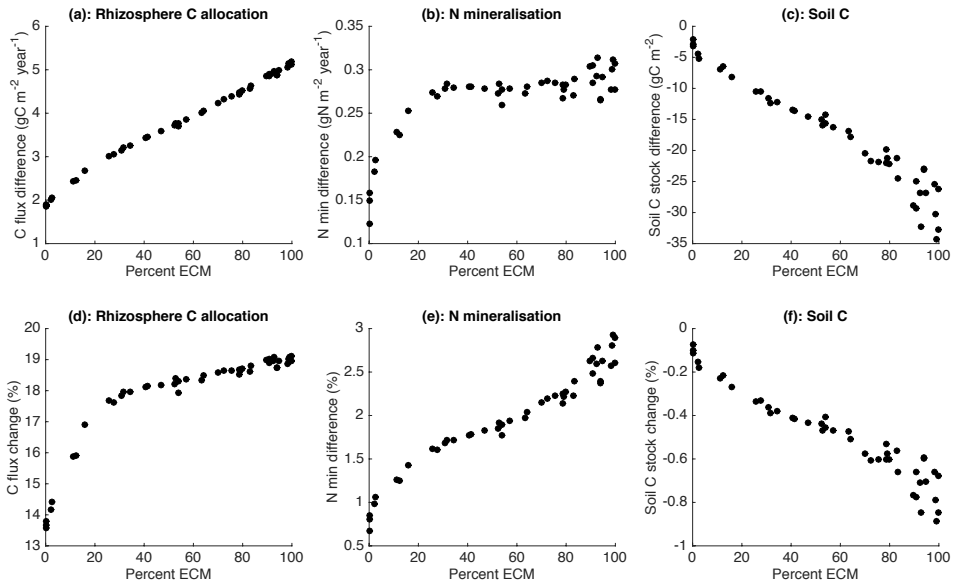

706

707 Figure 6: Responses to 20% increase in growth rates, as might be expected under

708 elevated CO_2. All plots show simulations with increased rhizosphere C allocation relative

709 to simulations with increased N demand and litter deposition but no change in

710 rhizosphere C allocation. Panels a-c show absolute changes, and panels d-f show percent

711 changes. a, d: Rhizosphere C allocation. b, e: Soil N mineralization rate. c, f: Soil C

712 stock.

713